

Article

Influence of Synthesis Parameters on the Structural and Superconducting Characteristics of $\text{Bi}_2\text{Sr}_2\text{Ca}_3\text{Cu}_4\text{O}_{10+\delta}$ High-Temperature Superconductors

Fatima Ali Hussein^{*1}, Sabah Jalal Fathi²

1,2. Department of Physics, College of Education for Pure Sciences, University of Kirkuk, Kirkuk, Iraq

* Correspondence: Scpm24011@uokirkuk.edu.iq

Abstract: This study investigates the influence of annealing temperature on the structural and superconducting characteristics of $\text{Bi}_2\text{Sr}_2\text{Ca}_3\text{Cu}_4\text{O}_{10+\delta}$ high-temperature superconductors synthesized using the solid-state reaction method. Samples were annealed at 650°C, 750°C, and 850°C in an oxygen-rich atmosphere to control phase formation, crystal structure, and superconducting behavior. X-ray diffraction (XRD) analysis confirmed a progressive transformation from low- CuO_2 -layer phases to the Bi-2234 phase, with an optimal c/a ratio and crystallite size observed at 850°C. Electrical measurements showed enhanced superconductivity at 850°C, with a sharp transition temperature ($T_{c(\text{on})} = 115.8 \text{ K}$) and narrow ΔT_c , indicating high phase purity. SEM and AFM analyses revealed improved grain connectivity, reduced surface roughness, and enhanced structural uniformity at elevated temperatures. The results confirm that 850°C is the optimal annealing temperature for achieving superior structural integrity and superconducting performance in Bi-2234 compounds.

Keywords: High- T_c Superconductivity, Bi-2234 phase Evolution, Thermal Annealing Optimization, Solid-State Synthesis Route, Crystallographic Phase Transformation, SEM, AFM, XRD

Citation: Hussein, F. A & Fathi, S. J. Influence of Synthesis Parameters on the Structural and Superconducting Characteristics of $\text{Bi}_2\text{Sr}_2\text{Ca}_3\text{Cu}_4\text{O}_{10+\delta}$ High-Temperature Superconductors. Central Asian Journal of Medical and Natural Science 2025, 6(4), 1740-1749.

Received: 30th Jun 2025

Revised: 07th Jul 2025

Accepted: 21st Jul 2025

Published: 03rd Aug 2025



Copyright: © 2025 by the authors. Submitted for open access publication under the terms and conditions of the Creative Commons Attribution (CC BY) license (<https://creativecommons.org/licenses/by/4.0/>)

1. Introduction

The physical characteristics of superconducting materials varies markedly across various substances, a discrepancy due to variations in their structural and electrical compositions [1]. The crucial temperature (T_c) at which a material transitions into the superconducting state varies according to the material type. The specific electrical resistance and the temperature at which standard electrical conductivity deteriorates also fluctuate [2]. Conversely, superconducting materials represent a unique category of physical substances, displaying characteristics that are contingent not only on the material type but also on certain external factors such as temperature, magnetic field, and current density. All superconducting materials possess a crucial characteristic: the total absence of electrical resistance upon attaining a designated critical temperature, together with the incapacity to let magnetic fields to infiltrate at low temperatures (the Meissner effect) [3], [4]. This state is characterized by three fundamental parameters that govern the behavior of superconducting materials: critical temperature (T_c) [5], critical magnetic field (H_c), and

critical current density (J_c) [6]. Each variable directly influences the stability of the superconducting state, with their values contingent upon the structural composition and ambient cooling conditions [7]. To attain superconductivity, the three parameters (T_c , H_c , J_c) must remain inside certain thresholds. If any of these thresholds are surpassed — due to elevated temperature, increased magnetic field, or excessive critical current density — the material forfeits its superconductivity and reverts to its conventional resistive condition [8], [9]. Superconductivity is a captivating phenomenon in solid-state physics, characterized by its atypical features that defy the typical behavior of materials under standard circumstances [10], [11]. When specific elements or compounds are cooled to extremely low temperatures, approaching a few kelvins, they demonstrate a total absence of electrical resistance, permitting electrical current to flow without any energy loss or heat dissipation, rendering them optimal for high-efficiency applications such as lossless electrical transmission and superconductors [12]. The temperature at which this transition occurs is termed the "critical temperature" (T_c), which varies across materials and mostly relies on their electrical structure and bonding network. Since then, the periodic table has undergone frequent revisions to discover elements or compounds that have superconducting properties at comparatively low or high temperatures [13], [14]. Superconductors with a critical temperature higher than 77 K that discovered in 1987 by [15].

2. Materials and Methods

2.1 Materials

Chemicals:

Pure chemicals with a purity of 99% were used to prepare the Bi-Sr-Ca-Cu-O system compounds, namely:

Bi_2O_3 Bismuth oxide

$\text{Sr}(\text{NO}_3)_2$ Strontium nitrate

CaO Calcium oxide

CuO Copper oxide

1. Isopropyl alcohol $\text{C}_3\text{H}_8\text{O}$ (Isopropyl Alcohol)

Used as a solvent and aid in the mixing process to achieve complete homogeneity between the powders.

2. Oxygen gas O_2

To provide a saturated oxidizing atmosphere during sintering and annealing processes.

2.2 Sample preparation methods

This section includes a detailed presentation of the practical aspect of the research, which involves the preparation of superconducting compounds from the Bi-Sr-Ca-Cu-O family, specifically the phase $(\text{Bi}_2\text{Sr}_2\text{Ca}_2\text{Cu}_3\text{O}_{10+\delta})$, using the solid-state reaction method (which involves combining oxides and nitrates of the primary elements in precisely calculated weight ratios, followed by a series of controlled heat treatments. Pre-sintering and final annealing were performed at multiple temperatures of 650°C, 750°C, and 850°C in an oxygen-saturated atmosphere to study the effect of heat treatment on the formation and stability of crystal phases. After initial sintering, the samples underwent a series of final thermal annealing processes at three different temperatures: 650°C, 750°C, and 850°C. Three different crystalline phases were prepared: Bi-2212, Bi-2234, and Bi-2235. Three separate samples were prepared for each phase, resulting in nine samples, each of which underwent annealing at 650°C, 750°C, and 850°C. Bi-2223, and Bi-2234. Three separate samples were prepared for each phase, resulting in nine samples, each of which was annealed at one of the three temperatures. The annealing process was carried out using a constant heating rate of 5°C/min from room temperature to the target annealing temperature. The final temperature was then held for 24 hours in an oxygen-saturated (O_2) atmosphere to maintain the stability of the copper and bismuth oxides, prevent reduction,

and promote the formation of the target crystalline phase. After completing the 24-hour annealing stage, all samples were gradually cooled inside the furnace using a constant cooling rate of 5°C per minute until reaching room temperature. This cooling rate was chosen based on the principle of controlling interstitial thermal contraction within the crystal lattice of superconducting compounds, as slow cooling reduces the likelihood of internal thermal stresses or microscopic cracks in the crystal structure, allowing the oxygen distribution in the layered structure to stabilize, which contributes to controlling the oxygen content necessary to achieve superconductivity, helps complete the interstitial crystal arrangement, and avoids reverse phase transitions resulting from rapid cooling. Gradual cooling has also been adopted to maintain the stability of the Cu^{2+} state within the copper layers, which prevents its unwanted reduction and preserves the superconducting properties acquired during annealing.

3. Results and Discussion

3.1 XRD Test Results

The crystal structure of $\text{Bi}_2\text{Sr}_2\text{Ca}_3\text{Cu}_4\text{O}_{10+\delta}$ samples was analyzed using X-ray diffraction (XRD) after annealing at different temperatures, as shown in Table (1) and Figure(1). The results showed a gradual improvement in crystallization quality with increasing temperature, with diffraction peaks becoming sharper and clearer at 850°C, indicating directed crystal growth and better crystallization. The diffraction patterns also indicated a gradual transition in the phase composition from the few-layer phases Bi-2201 and Bi-2212 to phases with a larger number of CuO_2 layers, such as Bi-2234, which is one of the most important phases associated with high-temperature superconductivity. Among the structural factors supporting this phase transition, the c/a ratio was an important structural factor through which the formation of phases with an elongated longitudinal axis could be inferred, as shown in Figure (2). A gradual increase in the c/a ratio was observed with increasing temperature, reaching 5.70 at 850 °C, which is the highest value recorded in the study. This increase is attributed to the elongation of the C axis length resulting from the introduction of additional layers of CuO_2 , which is a strong indicator of the growth of the Bi-2234 phase. This structural observation is consistent with the quantitative results, where the Bi-2234 phase reached 15% at 850 °C, compared to only 5% at 750°C and 2% at 650°C. As shown in Figure (), the results indicate that 850°C represents the optimal conditions for the growth of the Bi-2234 phase in the Bi-Sr-Ca-Cu-O system.

Table 1. Structural properties of surface samples (Sdr) for $\text{Bi}_2\text{Sr}_2\text{Ca}_3\text{Cu}_4\text{O}_{10+\delta}$ composite samples annealed at different temperatures.

c/a Ratio	c (Å)	b (Å)	a (Å)	Impurities (%)	Bi-2201 Phase (%)	Bi-2212 Phase (%)	Bi-2223 Phase (%)	Bi-2234 Phase (%)	Annealing Temp (°C)
5.55	30.2	5.44	5.44	24	28	40	6	2	650
5.6	30.7	5.42	5.48	10	10	65	10	5	750
5.7	31.2	5.43	5.47	6	5	50	10	15	850

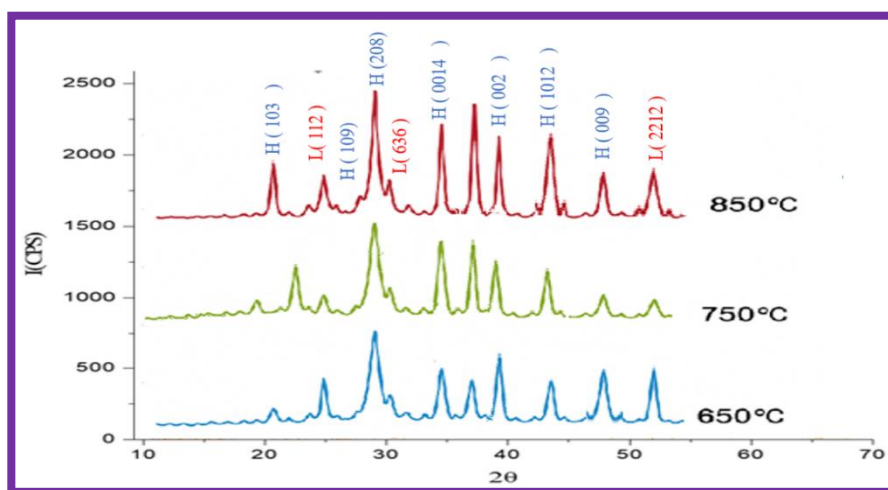


Figure 1. X-ray diffraction results for $\text{Bi}_2\text{Sr}_2\text{Ca}_3\text{Cu}_4\text{O}_{10+\delta}$ composite samples at different annealing temperatures.

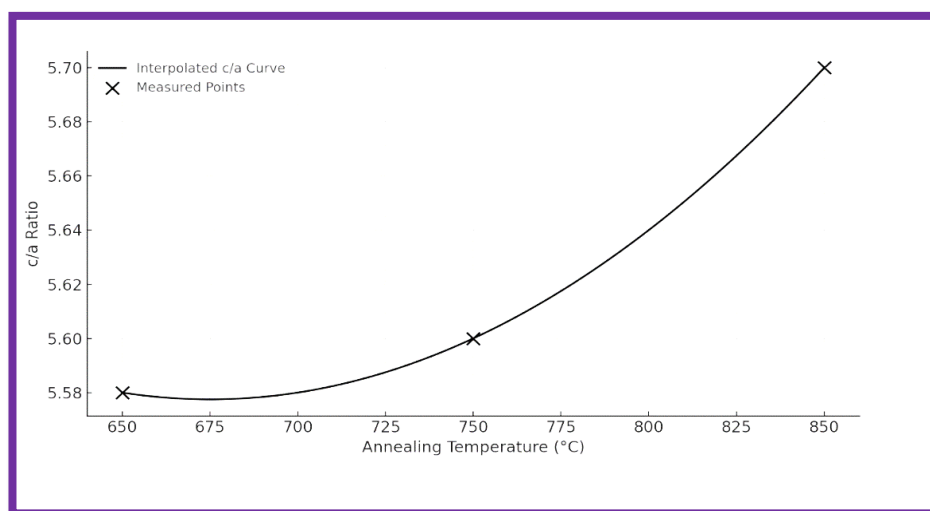


Figure 2. shows the values of c/a as a function of the annealing temperatures used in the preparation of $\text{Bi}_2\text{Sr}_2\text{Ca}_3\text{Cu}_4\text{O}_{10+\delta}$ composite samples.

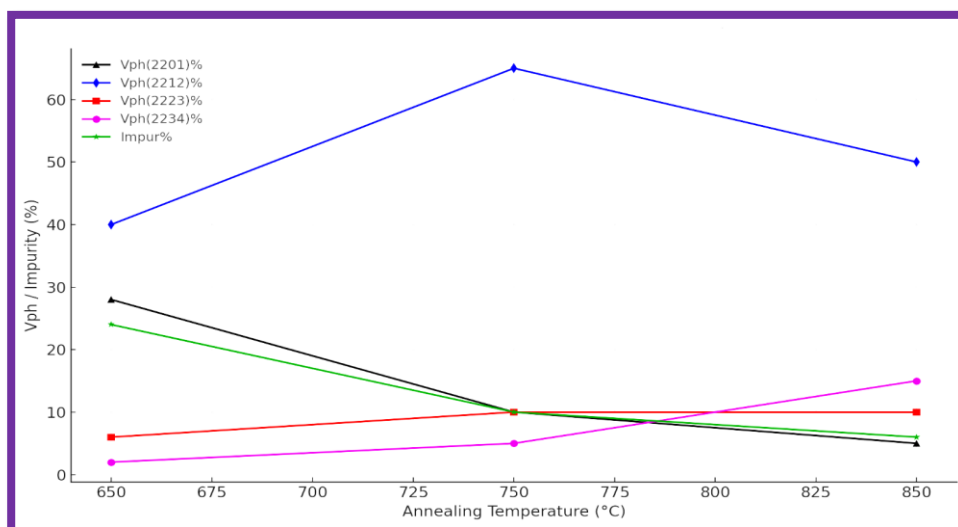


Figure 3. Change in phase ratios when preparing $\text{Bi}_2\text{Sr}_2\text{Ca}_3\text{Cu}_4\text{O}_{10+\delta}$ composite samples and impurity ratio as a function of sintering temperature.

The average crystallite size of the $\text{Bi}_2\text{Sr}_2\text{Ca}_3\text{Cu}_4\text{O}_{10+\delta}$ compound was calculated at three different annealing temperatures, as shown in Table 2 and Figure 3, using the Debye-Scherrer equation based on X-ray diffraction (XRD) data. The results showed that the crystallite size increased significantly with increasing annealing temperature, reaching 28.2 nm at 650 °C, rising to 35.5 nm at 750 °C, reaching a maximum value of 48.6 nm at 850°C. This regular increase indicates that sintering at higher temperatures improves crystallization and reduces grain boundaries and crystal defects, thereby enhancing the regularity of the Bi-2212 phase crystal lattice. The greater crystal growth at 850°C reflects optimal thermal conditions that allow for the rearrangement of atoms and reduction of internal stresses in the structure, supporting the formation of larger and more stable crystals. These results confirm that the annealing temperature of 850°C represents the optimal conditions for obtaining larger and more uniform crystal sizes for the Bi-2224 phase, which is an important indicator for improving the structural and electronic properties of the material.

Table 2. Average crystal size of $\text{Bi}_2\text{Sr}_2\text{Ca}_3\text{Cu}_4\text{O}_{10+\delta}$ samples at different annealing temperatures calculated using the Debye-Scherer equation.

Average Crystallite Size Dsh (nm)	Annealing Temperature (°C)
28.2	650
35.5	750
48.6	850

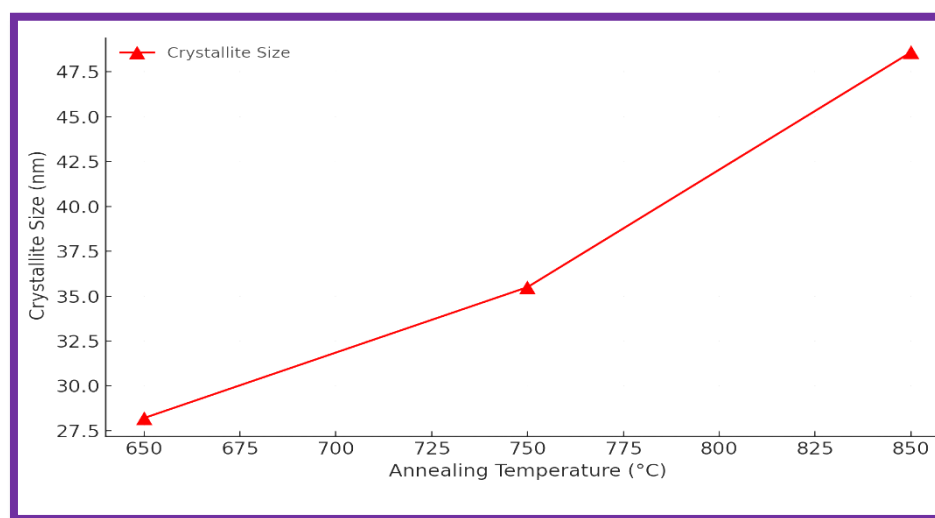


Figure 4. Crystal size as a function of melting temperatures for $\text{Bi}_2\text{Sr}_2\text{Ca}_3\text{Cu}_4\text{O}_{10+\delta}$ composite samples.

3.2 Electrical resistance results and critical temperature of the compound

The superconducting properties of the Bi-2234 sample prepared at three annealing temperatures, as shown in Table (3) and Figure (5), were studied by analyzing the resistance curves versus temperature. The three superconducting transition temperatures were extracted: the onset temperature $T_{(c(on))}^{\wedge}$ and the end temperature $T_{(c(off))}^{\wedge}$, in addition to the transition width ΔT_C and hole concentration p , as indicators of the quality of the superconducting phase. The results showed that the sample treated at 850°C achieved the highest superconducting performance, reaching $T_{(c(on))}^{\wedge}$ of 115.8 K, compared to the other samples, which recorded lower transition temperatures. Furthermore, the transition width ΔT_C was the lowest (3.2 K) at 850 °C, indicating a sharp and homogeneous transition to the superconducting state, which is an indicator of

the growth of a pure crystalline phase free of secondary phases. In terms of electronic structure, the p-hole concentration showed a gradual increase with increasing annealing temperature, as shown in Figure (6), reaching 0.160 at 850°C. This increase is related to the increased oxygen absorption in the structure, which improves the density of charge carriers (holes) in the CuO_2 levels, and thus enhances the superconducting properties of the Bi-2234 phase. These results clearly indicate that a temperature of 850°C is optimal for the formation of the Bi-2234 superconductor, Where the best characteristics of super transmission and uniform distribution of holes are achieved.

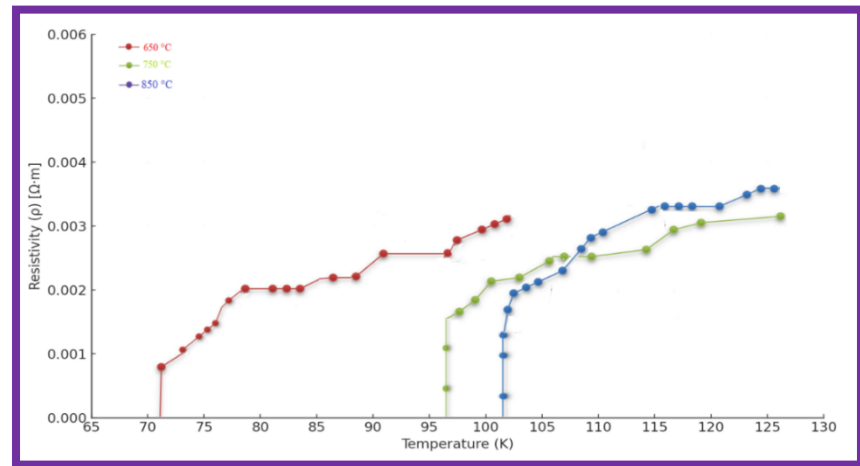


Figure 5. Shows the curves of the relationship between electrical resistance and temperature for samples of the $\text{Bi}_2\text{Sr}_2\text{Ca}_3\text{Cu}_4\text{O}_{10+\delta}$ compound annealed at different temperatures, illustrating the transition to the superconducting state for each sample.

Table 3. Critical temperatures and hole concentrations for $\text{Bi}_2\text{Sr}_2\text{Ca}_3\text{Cu}_4\text{O}_{10+\delta}$ composite samples at different annealing temperatures.

Hole Concentration (p)	ΔT_c (K)	$T_{c(off)}$ (K)	$T_{c(on)}$ (K)	Annealing Temperature (°C)
0.096	5.8	72.5	79.5	650
0.11797	4.6	96	101.2	750
0.14518	3.2	111.4	115.8	850

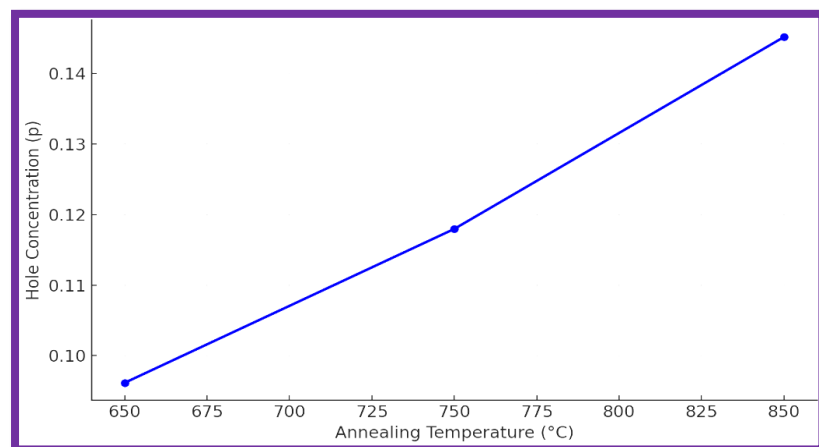


Figure 6. Relationship between hole concentration (p) and melting temperature for $\text{Bi}_2\text{Sr}_2\text{Ca}_3\text{Cu}_4\text{O}_{10+\delta}$ composite samples.

3.3 Results of SEM scanning electron microscope examination of the compound.

The surface structure of Bi-2234 samples was examined using a scanning electron microscope (SEM) to analyze the microscopic structural evolution resulting from thermal annealing at 650°C, 750°C, and 850°C, in support of the structural and electronic results obtained from XRD and electrical resistance measurements. The microscopic image of the (650°C) sample shown in Figure 7 revealed a heterogeneous surface structure containing small, irregularly distributed granular agglomerates, indicating limited crystalline growth and widespread interstitial voids. These features are consistent with the structural results, which indicated a low crystal size (28.2 nm) and a negligible Bi-2234 phase fraction (2%), in addition to a non-sharp supertransition and a low critical temperature.

Figure 8 (750°C) showed a marked improvement in crystallization regularity. The grains appeared more clearly with relative contact between the crystals, while retaining some grain boundaries. This corresponds to an increase in crystal size to 35.5 nm, improved pore concentration and phase purity, but the Bi-2234 phase is still in the process of partial formation. In contrast, Figure 9 (850°C) is characterized by a coherent and clear crystal structure, with large crystals with clean edges and uniform distribution in all directions. Clear grain merging can be observed as a result of atom rearrangement during high annealing. This image is a direct reflection of the significant improvement in the crystalline structure, supported by an increase in the Bi-2234 phase to 15%, a supercritical transition temperature of K 115.8, and an increase in crystal size to 48.6 nm. The high hole ratio ($p = 0.160$) indicates effective crystallization and a clear enhancement of superconductivity, supporting all previous structural and electronic conclusions.

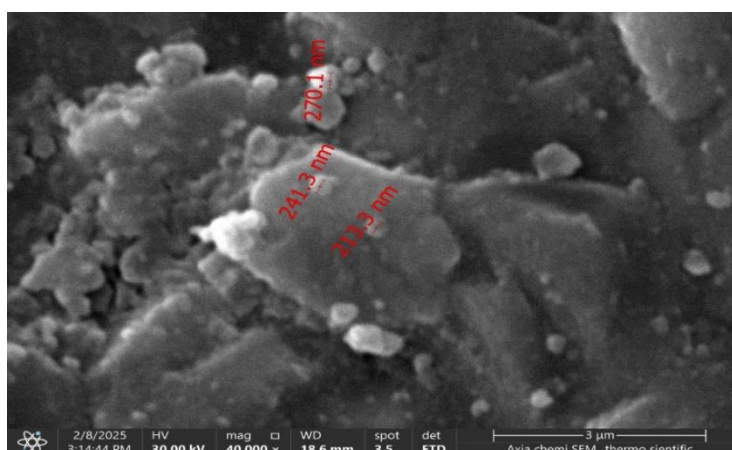


Figure 7. Scanning electron microscope image of the compound $\text{Bi}_2\text{Sr}_2\text{Ca}_3\text{Cu}_4\text{O}_{10-\delta}$ at a temperature of 650°C.

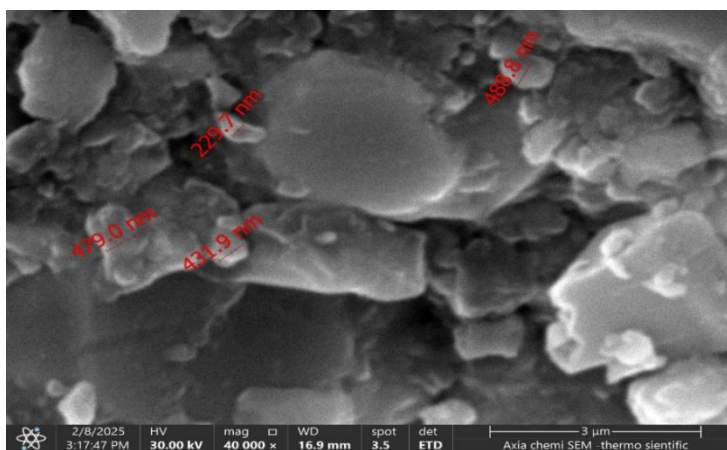


Figure 8. Scanning electron microscope image of the compound $\text{Bi}_2\text{Sr}_2\text{Ca}_3\text{Cu}_4\text{O}_{10-\delta}$ at a temperature of 750°C.

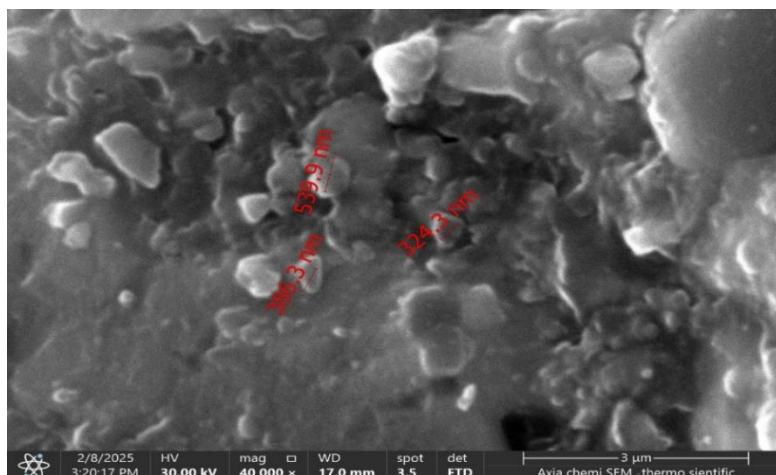


Figure 9. shows a scanning electron microscope image of the compound $\text{Bi}_2\text{Sr}_2\text{Ca}_3\text{Cu}_4\text{O}_{10+\delta}$ at a temperature of 850°C .

3.4 Results of atomic force microscopy (AFM) examination of the compound

The surface topography of Bi-2234 samples was analyzed using atomic force microscopy (AFM) to evaluate the effect of annealing temperature on surface properties, as shown in Figure (10). The analysis focused on the average surface roughness (S_a) and the effective surface area complexity ratio (Sdr) as indicators of crystal growth regularity and crystallization quality. At 650°C , the sample exhibited a rough surface structure with scattered peaks and sharp protrusions, with a non-uniform distribution of grains. The average surface roughness $S_a = 18.43 \text{ nm}$ and surface complexity ratio $\text{Sdr} = 6.21\%$ were recorded, indicating the presence of crystalline defects and irregular primary growth. These results are consistent with the small crystal size and poor superconducting properties of this sample. When annealed at 750°C , the surface regularity improved significantly, and the grains began to coalesce and converge, with a decrease in the severity of topographical variations. $S_a = 14.08 \text{ nm}$ and $\text{Sdr} = 3.87\%$ were obtained, reflecting the onset of more uniform crystal growth and relative development in the structural composition, which was confirmed by XRD and resistivity data. In the sample treated at 850°C , the surface was characterized by the highest degree of uniformity and smoothness, with the nanoparticles appearing clearly close together and evenly distributed across the surface. The surface roughness reached $S_a = 9.63 \text{ nm}$, while the surface complexity ratio decreased to $\text{Sdr} = 1.83\%$, reflecting effective atomic rearrangement and a significant improvement in crystallization. These high surface properties are in perfect agreement with the highest crystal volume, highest pore concentration, and best superconductor performance observed in this sample.

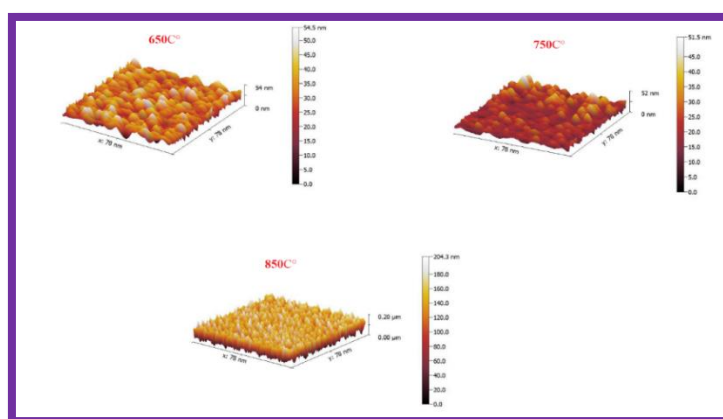


Figure 10. Atomic force microscope images of the $\text{Bi}_2\text{Sr}_2\text{Ca}_3\text{Cu}_4\text{O}_{8+\delta}$ compound at different annealing temperatures.

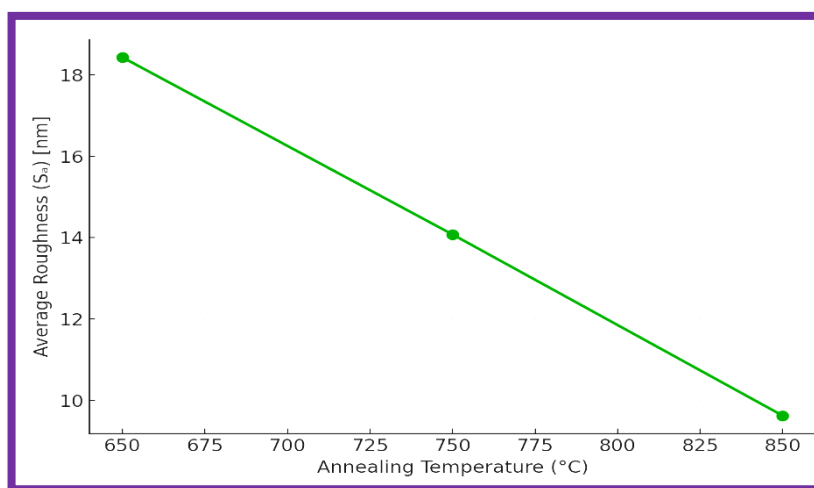


Figure 11. Relationship between annealing temperature and average surface roughness (Sa) for $\text{Bi}_2\text{Sr}_2\text{Ca}_3\text{Cu}_4\text{O}_{10+\delta}$ samples as measured using AFM.

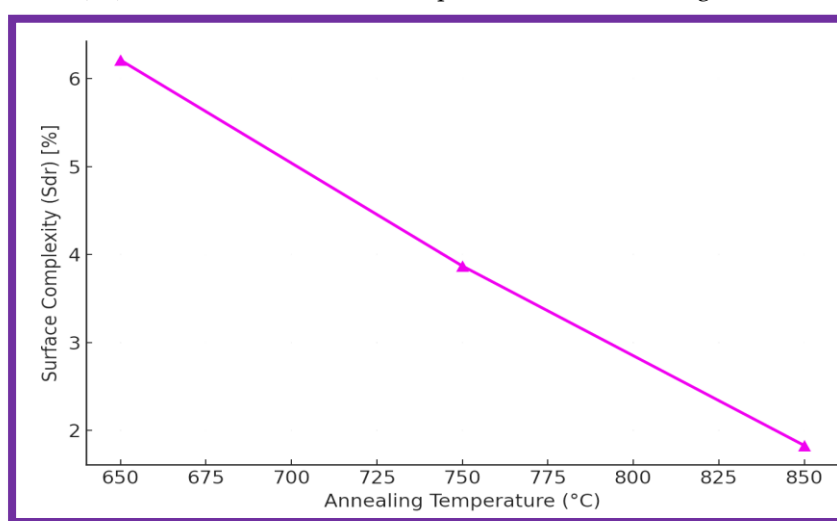


Figure 12. Relationship between the softening temperature and surface complexity ratio (Sdr) of $\text{Bi}_2\text{Sr}_2\text{Ca}_3\text{Cu}_4\text{O}_{10+\delta}$ composite samples as measured using AFM.

4. Conclusion

The findings of this study clearly demonstrate that annealing temperature plays a critical role in determining the structural and superconducting properties of $\text{Bi}_2\text{Sr}_2\text{Ca}_3\text{Cu}_4\text{O}_{10+\delta}$ compounds. The optimal annealing temperature was identified as 850°C, at which the Bi-2234 phase formation was maximized, exhibiting enhanced crystallinity, increased crystallite size, and a well-developed layered structure. XRD analysis confirmed the presence of sharper peaks and a higher c/a ratio, while electrical measurements revealed a superior superconducting transition with the highest onset temperature ($T_{c(\text{on})} = 115.8 \text{ K}$) and narrowest transition width ($\Delta T_c = 3.2 \text{ K}$). SEM and AFM results supported these findings by showing a homogeneous microstructure, increased grain connectivity, and minimal surface roughness. These improvements are attributed to better oxygen diffusion, enhanced phase purity, and reduced structural defects at higher temperatures. Overall, the study provides strong evidence that precise control of synthesis parameters, especially annealing temperature, is essential for optimizing the performance of high- T_c superconductors based on the Bi-Sr-Ca-Cu-O system.

REFERENCES

- [1] C. P. Poole, H. A. Farach, R. J. Creswick, and R. Prozorov, *Superconductivity*. Elsevier, 2014.
- [2] K. Onnes, "The resistance of pure mercury at helium temperatures," *Commun. Phys. Lab. Univ. Leiden*, b, vol. 120, 1911.
- [3] T. H. Glisson, *Introduction to circuit analysis and design*. Springer Science & Business Media, 2011.
- [4] K. A. Jasim, C. A. Z. Saleh, and A. H. A. Jassim, "Synthesis and Analysis of the Impact of Partial Mercury Replacement with Lead on the Structural and Electrical Properties of the $\text{Hg}_{1-x}\text{Pb}_x\text{Ba}_2\text{Ca}_2\text{Cu}_3\text{O}_{8+\delta}$ Superconductor," *Korean J. Mater. Res.*, vol. 34, no. 1, pp. 21–26, 2024.
- [5] B. Metin, N. Kavasoglu, and A. S. Kavasoglu, "AFORS-HET simulation for investigating the performance of $\text{ZnO}/\text{n-CdS}/\text{p-CdTe}/\text{Ag}$ solar cell depending on CdTe acceptor concentration and temperature," *Phys. B Condens. Matter*, vol. 649, p. 414504, 2023.
- [6] F. A. Karbarz *et al.*, "Synthesis of 85 K $\text{Bi}\otimes\text{Sr}\otimes\text{Ca}\otimes\text{Cu}\otimes\text{O}$ superconductor," *Mater. Res. Bull.*, vol. 25, no. 2, pp. 251–256, 1990.
- [7] 215–224. [38] Abbas, M. M., Abass, L. K., & Salman, U. (2012). Influences of sintering time on the TC of $\text{Bi}_{2-x}\text{Cu}_x\text{Pb}_{0.3}\text{Sr}_2\text{Ca}_2\text{Cu}_3\text{O}_{10+}$ high temperature superconductors. *Energy Procedia*, 18, "Influences of sintering time on the Tc of $\text{Bi}_{2-x}\text{Cu}_x\text{Pb}_{0.3}\text{Sr}_2\text{Ca}_2\text{Cu}_3\text{O}_{10+}$ δ high temperature superconductors," *Energy Procedia*, vol. 18, pp. 215–224, 2012.
- [8] A. R. Abdulridha, E. Al-Bermay, F. S. Hashim, and A. H. O. Alkhayatt, "Synthesis and characterization and pelletization pressure effect on the properties of $\text{Bi}_{1.7}\text{Pb}_{0.3}\text{Sr}_{2.0}\text{Ca}_2\text{Cu}_3\text{O}_{10+\delta}$ superconductor system," *Intermetallics*, vol. 127, p. 106967, 2020.
- [9] K. A. Jasim, R. A. A.-Z. Fadil, K. M. Wadi, and A. H. Shaban, "Partial Substitution of Copper with Nickel for the Superconducting Bismuth Compound and Its Effect on the Physical and Electrical Properties," *Korean J. Mater. Res.*, vol. 33, no. 9, pp. 360–366, 2023.
- [10] M. Tinkham, *Introduction to superconductivity*. Courier Corporation, 2004.
- [11] B. A. Omar, N. S. Abed, and A. S. Baqi, "Effects of La_2O_3 Nanoparticles on the Superconducting Behavior of $\text{Bi}_{1.60}\text{Ag}_{0.40}\text{Sr}_{1.9}\text{Ba}_{0.1}\text{Ca}_2\text{Cu}_3\text{O}_{10+\delta}$ Ceramics," *Sci. Technol. Sci. Soc.*, vol. 2, no. 6, pp. 75–82, 2025.
- [12] D. A. Cardwell, D. C. Larbalestier, and A. Braginski, *Handbook of Superconductivity: Characterization and Applications, Volume Three*. CRC Press, 2022.
- [13] O. F. de Lima, "THE RESEARCH ON SUPERCONDUCTIVITY IN BRAZIL," *Festschrift Honor Rogerio Cerqueira Leite*, p. 308, 1991.
- [14] A. Sergeev and I. Golev, "High-Temperature Superconducting Materials Based on Bismuth with a Low Critical Current," *Mater. Today Proc.*, vol. 11, pp. 489–493, 2019.
- [15] S. S. A. Alimardan, A. K. D. Ali, and S. J. Fathi, "Partial substitution Effect of Pb and Mg on the Structural and Electrical Properties of High Temperature ($\text{Hg}_{1-x}\text{Pb}_x\text{Ba}_2\text{Ca}_3\text{-yMg}_y\text{Cu}_4\text{O}_{10+\delta}$) Superconductor," *Tikrit J. Pure Sci.*, vol. 24, no. 2, pp. 68–87, 2019.